

UC Davis

UC Davis Previously Published Works

Title

From the Cover: BDE-47 and BDE-49 Inhibit Axonal Growth in Primary Rat Hippocampal Neuron-Glia Co-Cultures via Ryanodine Receptor-Dependent Mechanisms.

Permalink

<https://escholarship.org/uc/item/15j6965h>

Journal

Toxicological Sciences, 156(2)

ISSN

1096-6080

Authors

Chen, Hao

Streifel, Karin M

Singh, Vikrant

et al.

Publication Date

2017-04-01

DOI

10.1093/toxsci/kfw259

Peer reviewed

1 **BDE-47 and BDE-49 Inhibit Axonal Growth in Primary Rat Hippocampal Neuron-Glia**
2 **Co-Cultures via Ryanodine Receptor-Dependent Mechanisms**

3
4 Hao Chen*, Karin M. Streifel*, Vikrant Singh†, Dongren Yang*, Linley Mangini*, Heike Wulff†,
5 and Pamela J. Lein*‡

6
7 *Department of Molecular Biosciences, School of Veterinary Medicine, University of California-
8 Davis, Davis, CA 95616; haochen@ucdavis.edu; karin.streifel@gmail.com;
9 lmangini@ucdavis.edu; pjlein@ucdavis.edu; †Department of Pharmacology, School of
10 Medicine, University of California-Davis, Davis, CA 95616; vssingh@ucdavis.edu;
11 hwulff@ucdavis.edu

12
13 ‡Corresponding author: Pamela J. Lein, PhD
14 Molecular Biosciences, School of Veterinary Medicine
15 University of California, Davis
16 1089 Veterinary Medicine Drive
17 Davis, CA 95616
18 E-mail: pjlein@ucdavis.edu
19 Tel: (530) 752-1970
20 Fax: (530) 752-7690

21
22 Running Title: PBDEs inhibit axonal growth *in vitro*
23
24
25
26

27 **Abstract (limit is 250 words, currently at 250 words)**

28 Polybrominated diphenyl ethers (PBDEs) are widespread environmental contaminants
29 associated with adverse neurodevelopmental outcomes in children and preclinical models;
30 however, the mechanisms by which PBDEs cause developmental neurotoxicity remain
31 speculative. The structural similarity between PBDEs and non-dioxin-like (NDL) polychlorinated
32 biphenyls (PCBs) suggests shared toxicological properties. Consistent with this, both NDL
33 PCBs and PBDEs have been shown to stabilize ryanodine receptors (RyRs) in the open
34 configuration. NDL PCB effects on RyR activity are causally linked to increased dendritic
35 arborization, but whether PBDEs similarly enhance dendritic growth is not known. In this study,
36 we quantified the effects of individual BDE congeners on not only dendritic but also axonal
37 growth since both are regulated by RyR-dependent mechanisms, and both are critical
38 determinants of neuronal connectivity. Primary neuronal-glia co-cultures dissociated from the
39 neonatal rat hippocampus were exposed to BDE-47 or BDE-49 in the culture medium at
40 concentrations ranging from 20 pM to 2 μ M. At these concentrations, neither PBDE congener
41 altered dendritic arborization. In contrast, at concentrations \geq 200 pM, both congeners delayed
42 neuronal polarization resulting in significant inhibition of axonal outgrowth during the first few
43 days *in vitro*. The axon inhibitory effects of these PBDE congeners occurred independent of
44 cytotoxicity, and were blocked by pharmacological antagonism of RyR or siRNA knockdown of
45 RyR2. These results demonstrate that the molecular and cellular mechanisms by which PBDEs
46 interfere with neurodevelopment overlap with but are distinct from those of NDL PCBs, and
47 suggest that altered patterns of neuronal connectivity may contribute to the developmental
48 neurotoxicity of PBDEs.

49

50 **Keywords:** axon, calcium signaling, developmental neurotoxicity, neuronal morphogenesis,
51 PBDE, ryanodine receptor

52

53 **Introduction (750 word limit, currently at 655 words)**

54 Polybrominated diphenyl ethers (PBDEs), synthetic brominated compounds that were used
55 extensively as flame retardants in consumer products, have become persistent and ubiquitous
56 environmental contaminants. PBDE levels in human tissues have increased significantly over
57 the past three decades (EFSA, 2011; USEPA, 2010), and body burdens are significantly higher
58 in infants and toddlers relative to adults (Lunder *et al.*, 2010; She *et al.*, 2007; Toms *et al.*,
59 2009). Epidemiological studies report an association between early-life PBDE exposure and
60 neurobehavioral deficits, including decreased attention, poorer performance on intelligence
61 indices, psychomotor deficits and increased activity/impulsivity (Chao *et al.*, 2011; Eskenazi *et*
62 *al.*, 2013; Gascon *et al.*, 2012; Herbstman *et al.*, 2010; Hoffman *et al.*, 2012; Roze *et al.*,
63 2009; Shy *et al.*, 2011). Preclinical studies confirm that developmental PBDE exposures can
64 cause persistent neurobehavioral deficits (Costa *et al.*, 2014; Hendriks and Westerink, 2015).

65 PBDEs have been reported to interfere with thyroid hormone function, alter Ca^{2+}
66 homeostasis, cause oxidative stress and modulate cholinergic, glutamatergic and GABAergic
67 neurotransmission (Costa *et al.*, 2014; Dingemans *et al.*, 2011; Hendriks and Westerink,
68 2015). However, it is not clear whether or how these molecular effects relate to PBDE-induced
69 neurobehavioral deficits. One hypothesis is that PBDEs cause developmental neurotoxicity by
70 interfering with normal patterns of neuronal connectivity (Kodavanti and Curras-Collazo, 2010;
71 Stamou *et al.*, 2013). This hypothesis is derived from the following observations: (1) thyroid
72 hormone, Ca^{2+} , reactive oxygen species (ROS) and neurotransmitter-dependent signaling
73 mechanisms are well known to influence the development of neuronal connectivity via dynamic
74 control of axonal and dendritic morphogenesis (Chandrasekaran *et al.*, 2015; Goldberg, 2003;
75 Kapfhammer, 2004; Lohmann and Wong, 2005; Valnegri *et al.*, 2015); and (2) dysregulated
76 axonal or dendritic growth is linked to impaired behavior in preclinical models (Berger-Sweeney
77 and Hohmann, 1997), and to multiple neurodevelopmental disorders in humans, including

78 autism spectrum disorders, attention deficit hyperactivity disorder and schizophrenia (Copf,
79 2016; Robichaux and Cowan, 2014).

80 In further support of this hypothesis, we previously demonstrated that PBDE congeners with
81 more than one *ortho* bromine substitution interact with the ryanodine receptor (RyR) to promote
82 Ca^{2+} release from intracellular stores (Kim *et al.*, 2011). RyRs are Ca^{2+} channels that regulate
83 Ca^{2+} release from the endoplasmic reticulum (Pessah *et al.*, 2010), and RyR function is required
84 for activity-dependent dendritic growth (Adasme *et al.*, 2011; Ohashi *et al.*, 2014; Wayman *et*
85 *al.*, 2012b) and for axonal growth and guidance (Arie *et al.*, 2009; Gomez *et al.*, 1995;
86 Jacques-Fricke *et al.*, 2006; Ooashi *et al.*, 2005). Nanomolar concentrations of non-dioxin-like
87 (NDL) polychlorinated biphenyls (PCBs), which are structurally similar to PBDEs and proposed
88 to share toxicological modes of action (Kodavanti and Curras-Collazo, 2010), also interact with
89 RyR1 and RyR2 to sensitize their activation by submicromolar levels of Ca^{2+} and attenuate their
90 inhibition by micromolar levels of Ca^{2+} and Mg^{2+} (Wong *et al.*, 1997a; Wong and Pessah, 1996).
91 NDL PCB interactions with RyR stabilize the receptor in its open configuration (Samso *et al.*,
92 2009), which increases intracellular levels of Ca^{2+} (Wayman *et al.*, 2012a). NDL PCB
93 sensitization of RyRs is causally linked to enhanced dendritic arborization in hippocampal and
94 cortical neurons (Wayman *et al.*, 2012b; Yang *et al.*, 2014; Yang *et al.*, 2009) via activation of
95 Ca^{2+} -dependent signaling pathways (Wayman *et al.*, 2012a). While PBDEs were recently
96 reported to alter axonal growth in larval zebrafish (Chen *et al.*, 2012), whether PBDEs influence
97 axonal or dendritic morphogenesis in mammalian central neurons via RyR-dependent
98 mechanisms has not been previously evaluated.

99 Here, we address this question by exposing primary cultures of rat hippocampal neurons to
100 either BDE-47, a PBDE congener with weak RyR activity (Kim *et al.*, 2011) that is highly
101 abundant in human tissues (USEPA, 2010), or BDE-49, a PBDE congener with potent RyR
102 activity (Kim *et al.*, 2011) that has been detected in gestational tissues from women in southeast
103 Michigan at levels comparable to BDE-47 (Miller *et al.*, 2009). Our findings indicate that while

104 neither congener alters dendritic arborization, both decrease axonal growth with comparable
105 potency via RyR-dependent mechanisms.

106

107 **Materials and Methods**

108

109 **Materials**

110 Neat certified BDE-47 (2,2',4,4'-tetrabromodiphenyl ether, > 99% pure) and BDE-49 (2,2',4,5'-
111 tetrabromodiphenyl ether, > 99% pure) were purchased from AccuStandard Inc. (New Haven,
112 CT), and verified for purity and composition by GC/MS by the UC Davis Superfund Research
113 Program Analytical Core. Stock solutions of each BDE were made in dry dimethyl sulfoxide
114 (DMSO, Sigma-Aldrich, St. Louis, MO). Paraformaldehyde was purchased from Sigma-Aldrich.
115 FLA365 (4-(2-aminopropyl)-3,5-dichloro-*N,N*-dimethylaniline) was synthesized as previously
116 described (Florvall *et al.*, 1977) and confirmed to be > 99% pure by NMR (see Supplemental
117 File 1). Xestospongin C was purchased from Cayman Chemical (Ann Arbor, MI); verapamil,
118 from Sigma-Aldrich. MAP2B-eGFP and pCAG-tomato fluorescent protein (TFP) constructs were
119 generous gifts from Dr. Gary Wayman (Washington State University, Pullman, WA) and their
120 synthesis and characterization have been previously published (Wayman *et al.*, 2006).

121

122 **Animals**

123 All procedures involving animals were conducted according to protocols approved by the
124 Institutional Animal Care and Use Committee of the University of California, Davis. Timed-
125 pregnant Sprague Dawley rats were purchased from Charles River Laboratory (Hollister, CA)
126 and individually housed in clear plastic cages with corn cob bedding. Food and water were
127 provided *ad libitum*. Temperatures were maintained at 22 ± 2 °C throughout a 12 h light-dark
128 cycle.

129

130 **Cell Culture**

131 Primary hippocampal cell cultures were prepared from postnatal day (P) 0 or P1 male and
132 female rat pups (hippocampi from male and female pups were pooled) as previously described
133 (Wayman et al., 2006). Briefly, dissociated hippocampal cells were plated on glass coverslips
134 (Bellco Glass, Vineland, NJ) precoated with poly-L-lysine (0.5 mg/mL, Sigma-Aldrich) and
135 maintained at 37°C in NeuralQ Basal Medium supplemented with 2% GS21 (MTI-GlobalStem,
136 Gaithersburg, MD) and GlutaMAX (ThermoScientific, Waltham, MA). For studies of neuronal cell
137 polarization, axonal morphogenesis and intracellular Ca^{2+} levels, cells were plated at 33,000
138 cells/cm²; for studies of dendritic growth, at 83,000 cells/cm². Phase contrast images of cultures
139 grown at either cell density are provided in Supplemental Figure 2. For all PBDE exposure
140 experiments, cultures were exposed to varying concentrations of BDE-47 or BDE-49 diluted in
141 culture medium from 1000X stocks; control cultures were exposed to vehicle (DMSO; 1:1000
142 dilution). For studies of neuronal cell polarization, axonal growth and intracellular Ca^{2+} levels,
143 cultures were exposed for 48 h beginning 3 h after plating; for dendritic growth studies, cultures
144 were exposed for 48 h beginning on day *in vitro* (DIV) 7.

145

146 **siRNA Knockdown**

147 Construct sequences and specificity of RyR1 siRNA, RyR2 siRNA and control (scrambled)
148 siRNA were previously published (Wayman et al., 2012b). In this study, siRNA were
149 fluorescently labeled using LabelIT® (Mirus, Madison WI) per the manufacturer's instructions in
150 order to identify transfected cells. To transfect hippocampal neurons, freshly dissociated
151 hippocampal cells were electroporated with siRNA prior to plating using the Amaxa Nucleofector
152 (Amaxa Biosystems, Lonza) according to the manufacturer's protocol. Transfection efficiency
153 was approximately 40%.

154

155

156 ***Morphometric analyses***

157 To visualize the dendritic arbor, hippocampal cultures were transfected on DIV 6 with a
158 pCAGGS expression vector encoding a microtubule-associated protein-2B (MAP2B)-enhanced
159 green fluorescent protein (eGFP) fusion construct (Wayman et al., 2006), using Lipofectamine-
160 2000 (Invitrogen, Carlsbad, CA) according to the manufacturer's protocol. **Transfection**
161 **efficiency ranged between** Dendritic lengths were quantified from digital images of GFP+
162 neurons using ImageJ software with the NeuronJ plugin (Meijering *et al.*, 2004) by an individual
163 blinded to experimental condition. Total dendritic length was measured in at least 30 neurons
164 from 3 coverslips per treatment group, and the experiment was repeated at least three times
165 with cultures prepared from independent dissections.

166 To quantify axonal morphology, cultures were fixed with 4% paraformaldehyde then reacted
167 with antibody specific for Tau-1 (1:1000, Millipore, Billerica, MA) to visualize axons. Axonal
168 lengths were quantified in Tau-1 immunopositive neurons by an individual blinded to
169 experimental condition using ImageJ software with the NeuronJ plugin. As previously defined
170 (Dotti *et al.*, 1988; Lein *et al.*, 1992), a neurite was considered an axon if its length was at least
171 2.5 times the diameter of the cell body, and it exceeded in length all other neurites extended by
172 the same neuron. Total axonal length was measured in at least 30 neurons from 3 coverslips
173 per treatment group, and the experiment was repeated in cultures prepared from three
174 independent dissections.

175 To assess neuronal cell polarity, cultures were reacted with GAP-43 antibody (1:1000,
176 Millipore, Billerica, MA). Polarity was scored in GAP-43 immunopositive neurons by an
177 individual blinded to treatment using previously described stages (Goslin *et al.*, 1990). The
178 experiment was repeated in cultures prepared from three independent dissections.

179

180

181 ***Cytotoxicity Analyses***

182 Cytotoxicity was assessed by quantifying lactate dehydrogenase (LDH) released into the
183 culture medium (Mosmann, 1983) using the CytoTox-ONE™ Homogenous Membrane Integrity
184 Assay (Promega, Madison, WI, USA) per the manufacturer's directions. Cell viability was also
185 assessed in independent cultures by reacting cultures with calcein-AM (0.25 μM; Invitrogen) and
186 propidium iodide (1.25 μM; Sigma-Aldrich) to identify live and dead cells, respectively. The
187 percentage of live (calcein-AM labeled) versus dead (propidium iodide-labeled) cells in each
188 culture was determined using an automated high content imaging system (ImageExpress,
189 Molecular Devices, Sunnyvale, CA). Cytotoxicity was assayed in 12 wells per treatment and
190 experiments were repeated using cultures obtained from three independent dissections.

191

192 ***Western blot analysis of tau-1***

193 At DIV 5, low density cultures were treated with BDE-47 or BDE-49 for 48 h, then lysed with
194 ice-cold RIPA buffer (150 mM NaCl, 1.0% NP-40, 0.5% sodium deoxycholate, 0.1% SDS in 50
195 mM Tris, pH 8.0 with Halt protease inhibitor). Protein concentrations of the lysates were
196 determined using the BCA Protein Assay (Pierce, Rockford IL). An equal amount of protein (10
197 μg) of each sample was separated by 12% SDS-PAGE, and transferred to PDVF membrane.
198 Membranes were blocked for 1 h in Odyssey Blocking Buffer (LI-COR, Lincoln NE) then
199 incubated overnight with antibodies specific for tau-1 (1:1000, Millipore, Billerica, MA) and
200 GAPDH (1:1000, Cell Signaling Technology Danvers, MA) prepared in blocking buffer. After
201 PBS wash, membranes were incubated with secondary antibodies conjugated to infrared dye
202 IR700 or IR800 for 1 h and then washed with PBS. Membranes were scanned and
203 densitometric values obtained using the Odyssey Infrared Imaging System (LI-COR, Lincoln
204 NE). The densitometric value for each tau-1 immunopositive band was normalized to the
205 densitometric value for the GAPDH immunopositive band within the same sample.

206

207 ***Calcium Imaging***

208 Spontaneous Ca^{2+} transients were measured in dissociated hippocampal cells cultured on
209 CoStar® 96-well plates (Corning Inc, Corning, NY). At DIV 2, cells were loaded with the Ca^{2+} -
210 sensitive dye Fluo-4 AM (4 μM ; Invitrogen) in Locke's buffer (8.6 mM 4-(2-hydroxyethyl)-1-
211 piperazineethanesulfonic acid, 5.6 mM KCl, 154 mM NaCl, 5.6 mM glucose, 1.0 mM MgCl_2 , 2.3
212 mM CaCl_2 , and 0.0001 mM glycine, pH 7.4) at 37°C for 30 min. Cultures were washed with
213 Locke's Buffer and transferred to the ImageXpress Micro XLS high content imaging system. The
214 temperature was maintained at 37°C throughout the recording period. Fluorescence was
215 recorded every 15 s over the 26 min experiment. After 5 min of baseline recording, vehicle,
216 BDE-47 or BDE-49 was added to the cultures and data captured for an additional 20 min. At the
217 conclusion of the 20 min recording, viable neurons were identified by adding 30 mM KCl to the
218 medium to depolarize neurons; any neurons that did not respond with a transient Ca^{2+} spike
219 were not included in the subsequent analyses. The transient amplitude of Ca^{2+} fluorescence
220 was measured by normalizing peak change in Fluo-4 AM fluorescence (ΔF) to the baseline
221 fluorescence (F_0) and presented as the mean $\Delta F/F_0$ per neuron. Area under the curve (AUC)
222 measurements were calculated via the trapezoid method using Graphpad Prism version 4.0
223 (San Diego, CA). Baseline levels were held constant at zero and peaks less than 10% of total
224 amplitude were excluded. Levels of calcium flux within each cell were collected throughout the
225 experimental time from all treatments. Within each field of view, > 30 cells were identified for
226 analysis; 1 field was imaged per well in 2 wells per experimental group. Statistical comparisons
227 were made on mean values per group with cultures obtained from four independent dissections
228 (e.g., N=4 per group).

229

230 ***Immunocytochemical localization of RyR***

231 To confirm RyR expression in the axonal growth cone, cultures were fixed with 4%
232 paraformaldehyde on DIV 2, permeabilized with 0.1% Triton X-100 for 5 min, incubated in

233 blocking buffer containing 5% fetal bovine serum, 0.05 M NH₄Cl, 2% glycerol, and 2% goat
234 serum for 1 h and then reacted overnight with RyR1-selective antibody 34C (1:100,
235 Developmental Studies Hybridoma Bank, Iowa City, IA) or RyR2-selective antibody C3-33
236 (1:100, Abcam, Cambridge, MA). After PBS wash, Alexa Fluor dyes (1:1000, Molecular Probes,
237 Invitrogen) and Oregon-Green phalloidin (1:1000, ThermoScientific) were applied for 1 h.

238

239 ***Statistical analysis***

240 All data are presented as mean ± SE. Graphs and statistical analyses were performed with
241 GraphPad Prism 4.0. Data were analyzed using one-way ANOVA with Tukey's or Dunnett's
242 *post-hoc* or with Kruskal-Wallis with Dunn's *post-hoc* as appropriate. Datasets were log
243 transformed for statistical analysis if they did not pass the Shapiro-Wilk test of normality.

244

245 **Results**

246 ***BDE-47 and BDE-49 selectively interfere with axonal growth in primary hippocampal*** 247 ***neurons***

248 We have previously shown that RyR-active NDL-PCBs enhance dendritic arborization in
249 cultured hippocampal neurons (Wayman et al., 2012b; Yang et al., 2014). Therefore, we initially
250 predicted that BDE-47 and BDE-49, which exhibit relatively low versus relatively high RyR
251 activity, respectively (Kim et al., 2011), would exhibit weak versus robust dendrite promoting
252 activity. To visualize dendritic arbors of individual neurons in high-density neuron-glia co-
253 cultures dissociated from P0-P1 rat hippocampi, cultures were transfected with a MAP2B-EGFP
254 construct under the control of the neuron-specific CAG promoter (Wayman et al., 2006).
255 Expression of MAP2B-eGFP is restricted to the somatodendritic compartment in cultured
256 hippocampal neurons and does not alter their intrinsic dendritic growth patterns (Wayman et al.,
257 2006). Under the culture conditions used for these experiments, the dendritic arbor expands
258 most rapidly between DIV 5-10 (Wayman et al., 2006); therefore, cultures were transfected with

259 MAP2B-eGFP on DIV 6, then exposed from DIV 7-9 to varying concentrations of BDE-47 or
260 BDE-49. Control cultures were exposed to vehicle (DMSO at 1:1000 dilution) or, as a positive
261 control, to PCB 95 (200 nM). PCB 95 is a NDL-PCB with potent activity at the RyR that we
262 previously demonstrated significantly enhances dendritic arborization in cultured hippocampal
263 neurons (Wayman et al., 2012b). Consistent with previous studies (Wayman et al., 2012b),
264 neurons exposed to PCB 95 had a more complex dendritic arbor (Figure 1A), evidenced as a
265 significant increase in total dendritic length per neuron relative to vehicle control neurons (Figure
266 1B). In contrast, the dendritic arborization of neurons exposed to either BDE-47 or BDE-49 at
267 concentrations ranging from 200 pM to 2 μ M was not significantly different from that of neurons
268 exposed to vehicle (Figure 1A, B).

269 RyRs are expressed not only in dendrites (Seymour-Laurent and Barish, 1995; Wayman et
270 al., 2012b), but also in axons (Hertle and Yeckel, 2007), and RyR activity has been implicated in
271 the regulation of axonal growth and guidance (Ooashi et al., 2005; Welshhans and Rehder,
272 2007). Therefore, we examined whether PBDEs alter axonal growth in primary hippocampal
273 neurons. For studies of axonal growth, primary hippocampal cell cultures were plated at a lower
274 cell density and exposed to BDE-47 or BDE-49 for 48 h beginning 3 h after plating in order to
275 visualize the complete axonal plexus of individual neurons (Yang et al., 2014). At the end of the
276 exposure period, cultures were fixed and immunostained for tau-1, which is an axon-selective
277 cytoskeleton-associated protein (Hayashi *et al.*, 2002). Exposure to either BDE-47 or BDE-49
278 did not change the number of axons extended by cultured hippocampal neurons but did
279 significantly decrease the length of axons (Figure 2A). Morphometric analyses indicated that at
280 concentrations ranging from 200 pM to 2 μ M, both PBDE congeners significantly decreased
281 axonal length by 15-25% relative to vehicle control values (Figure 2B). Exposure to BDE-47 or
282 BDE-49 at 20 pM did not significantly alter axonal length relative to vehicle controls.

283 To determine whether PBDE effects on axonal growth are a secondary effect of cytotoxicity,
284 cell viability was assessed in PBDE-exposed cultures using two assays that measure different

285 parameters of cell health: LDH release (Lobner, 2000) and cellular uptake of calcein AM and
286 propidium iodide (Vaughan *et al.*, 1995). Under the same culture conditions and PBDE
287 exposure paradigms used for axonal growth studies, neither BDE-47 nor BDE-49 significantly
288 altered LDH release (Figure 3A) or calcein AM and propidium iodide uptake (Figure 3B) relative
289 to vehicle controls.

290 To determine whether the differential effects of BDE-47 and BDE-49 on axonal vs. dendritic
291 growth reflect differential susceptibility of immature (DIV 2) vs. more mature (DIV 7-9) cell
292 cultures, respectively, we tested the effects of these PBDE congeners on axonal growth
293 following the same exposure paradigm used for the dendritic growth assay. Because it is
294 technically challenging to quantify axonal lengths of individual neurons in mature cultures using
295 morphometric analyses, we used western blotting to quantify expression levels of the axon-
296 selective cytoskeletal protein tau-1 in hippocampal cultures exposed to BDE-47 or BDE-49 from
297 DIV 7-9. Levels of tau-1 protein in BDE-exposed cultures were not significantly different from
298 those in vehicle control cultures (Figure 4).

299 The observation that PBDEs did not significantly alter tau-1 expression in mature neurons
300 but did decrease axonal length in immature neurons (Figure 2) suggests that these compounds
301 interfere with very early events of axonal morphogenesis in hippocampal neurons. Previous
302 studies have shown that hippocampal neurons in culture undergo a well-defined sequence of
303 morphological changes to transition from an unpolarized cell with multiple “minor” neurites that
304 are neither axonal or dendritic into the characteristic polarized neuron with a single axonal
305 process and multiple dendrites (Dotti *et al.*, 1988). Polarization of these neurons typically occurs
306 over the first 24-48 h in culture, and is marked by the differentiation of one of multiple “minor”
307 neurites into a definable axon (Wiggin *et al.*, 2005). To assess whether PBDE effects on axon
308 length were mediated by changes in the rate of neuronal cell polarization, hippocampal cell
309 cultures were immunostained for GAP-43, a biomarker of axonal growth cones (Goslin and
310 Banker, 1990; Goslin *et al.*, 1990). To score the different stages of neuronal cell polarization,

311 we used previously described criteria based on neuronal cell morphology and the subcellular
312 distribution of GAP-43 immunoreactivity (Goslin and Banker, 1990; Goslin et al., 1990; Harrill
313 *et al.*, 2013). Briefly, polarization was scored as Stage 1 if GAP-34 immunoreactivity was
314 localized to the cell body with no discernable immunostaining of neurites; Stage 2, if GAP-43
315 immunoreactivity was obvious in all neurites and no one neurite was significantly longer than the
316 others; or Stage 3, if GAP-43 immunoreactivity was most robust in the growth cone of a single
317 neurite that was significantly longer than the remaining neurites (Figure 5A). Stage 3 marks the
318 initial polarization of the neuron when the GAP-43 immunopositive neurite becomes the axon
319 (Dotti et al., 1988; Goslin and Banker, 1990). Under the culture conditions used for our studies
320 of PBDE effects on axonal growth, the majority of neurons (> 75%) reached Stage 3, or become
321 polarized, within 48 h after plating (Figure 5B). Therefore, in experiments examining the effects
322 of PBDE exposure on neuronal cell polarization, we examined cultures at DIV 2. In cultures
323 exposed to either BDE-47 or BDE-49 at 200 nM for 48 h beginning 3 h after plating, there were
324 significantly fewer neurons that had reached stage 3 (or become polarized) by DIV 2 relative to
325 vehicle control cultures (Figure 5C).

326

327 ***PBDE effects on axonal growth are mediated by RyR-dependent mechanisms***

328 Cytosolic Ca^{2+} plays an important role in axonal growth and guidance (Zheng and Poo,
329 2007). Since it has previously been shown that PBDEs disrupt Ca^{2+} homeostasis (Dingemans *et*
330 *al.*, 2010b; Dingemans et al., 2011; Kim et al., 2011), we hypothesized that PBDE effects on
331 axonal growth are mediated by changes in intracellular Ca^{2+} levels ($[\text{Ca}^{2+}]_i$). To test this
332 hypothesis, hippocampal neurons at DIV 2 were acutely exposed to vehicle or concentrations of
333 BDE-47 or BDE-49 that inhibit axonal growth. At 2 nM or 2 μM , neither PBDE congener elicited
334 changes in $[\text{Ca}^{2+}]_i$ that were detectable using high content imaging of cells loaded with Fluo-4
335 AM (Supplemental file 3). To confirm that our approach was sensitive enough to detect
336 previously reported changes in $[\text{Ca}^{2+}]_i$ following acute exposures to higher PBDE concentrations

337 (Dingemans *et al.*, 2010a; Dingemans *et al.*, 2011), we quantified the effects of acute
338 exposures to BDE-47 or BDE-49 at 20 μM on $[\text{Ca}^{2+}]_i$ (Figure 5A). Both PBDE exposures
339 significantly increased $[\text{Ca}^{2+}]_i$ in the neuronal soma relative to vehicle controls as quantified by
340 the maximum amplitude of transient $[\text{Ca}^{2+}]$ spikes, and the area under the curve (Figure 5B).
341 Ca^{2+} transients localized to axonal growth cones were significantly increased by acute exposure
342 to BDE-47 but not BDE-49 (Figure 5C).

343 As an alternate approach for determining whether the inhibitory effects of PBDE on axonal
344 growth are mediated by Ca^{2+} -dependent mechanisms, we used pharmacological antagonists to
345 investigate the role of various Ca^{2+} ion channels in PBDE neurotoxicity. Hippocampal cultures
346 were pre-incubated 30 min prior to PBDE treatment with the L-type voltage Ca^{2+} channel
347 blocker verapamil (30 μM), the IP_3 receptor blocker xestospongine C (1 μM) or the RyR blocker
348 FLA365 (10 μM). These concentrations of verapamil (Keith *et al.*, 1994; Kodavanti *et al.*, 1994),
349 xestospongine C (Gafni *et al.*, 1997; Inglefield *et al.*, 2001) and FLA365 (Chiesi *et al.*, 1988;
350 Mack *et al.*, 1992) have previously been shown to block neuronal Ca^{2+} signaling. In the absence
351 of PBDEs, none of these pharmacological blockers altered basal levels of axonal growth relative
352 to vehicle controls (Figure 7A). Pretreatment of PBDE-exposed cultures with either verapamil or
353 xestospongine did not prevent the inhibitory effects of BDE-47 and BDE-49 on axonal growth; in
354 contrast, pretreatment with FLA365 blocked the inhibitory effects of both PBDE congeners on
355 axonal growth (Figure 7B).

356 FLA365 selectively blocks RyR Ca^{2+} channels, but has been reported to also interfere with
357 L-type Ca^{2+} channels in arterial smooth muscle cells (Ostrovskaya *et al.*, 2007). Therefore, to
358 confirm that FLA365 antagonizes the axon inhibiting activity of PBDEs via RyR Ca^{2+} channel
359 blockade, we determined whether siRNA knockdown of RyR phenocopies FLA365 treatment.
360 While all three RyR isoforms are expressed in the brain, we had previously shown that RyR1
361 and RyR2 are predominantly expressed in primary neuron-glia co-cultures derived from P0-1 rat
362 hippocampi (Wayman *et al.*, 2012b). To determine whether these two RyR isoforms are

363 expressed in axonal growth cones, DIV 2 hippocampal cultures were immunostained using
364 antibodies selective for RyR1 or RyR2 and co-labeled with phalloidin to identify axonal growth
365 cones. Puncta immunoreactive for both RyR1 and RyR2 were obvious throughout the cytoplasm
366 of the axonal growth cone and even out along the tips of the phalloidin-labeled filopodia (Figure
367 8A). Expression of RyR1, RyR2 or scrambled (control) siRNA did not alter axon length in vehicle
368 control cultures. In cultures exposed to PBDEs, expression of the control siRNA did not block
369 the axon inhibitory effect of BDE-47 or BDE-49. In contrast, expression of RyR2 siRNA blocked
370 inhibitory effects of both BDE-47 and BDE-49 on axon length (Figure 8B). Expression of RyR1
371 siRNA appeared to partially block the inhibitory effect of these PBDEs on axon growth as
372 evidenced by the fact that axon lengths of PBDE-exposed neurons expressing RyR1 siRNA
373 were not significantly different from either vehicle control neurons expressing RyR1 siRNA or
374 PBDE-exposed neurons expressing control siRNA.

375

376 **Discussion (Word Limit: 1500; currently at 1489 words)**

377 Our findings support the hypothesis that PBDEs cause developmental neurotoxicity by
378 interfering with cellular and molecular mechanisms that regulate neuronal connectivity in the
379 developing brain. Specifically, our data demonstrate that BDE 47 and BDE 49 inhibit the early
380 stages of axonal growth in primary cultures of perinatal rat hippocampal neurons. These data
381 extend previous reports demonstrating that commercial PBDE mixture, DE-71, decreases
382 neurite length in primary mouse cortical cultures (Bradner *et al.*, 2013), and that BDE-47 inhibits
383 neurite outgrowth in human embryonic stem cell-derived neurons (Behl *et al.*, 2015), and
384 decreases the length of axons of motor neurons in larval zebrafish (Chen *et al.*, 2012). In our
385 model, exposure to BDE-47 or BDE-49 significantly inhibits axonal growth at concentrations that
386 have no effect on cell viability, indicating that decreased axonal growth is not due to
387 compromised cell viability. Exposure of hippocampal cultures to the same concentration range
388 of BDE-47 or BDE-49 does not alter dendritic arborization. This suggests that PBDEs do not

389 inhibit general mechanisms of neurite outgrowth, but rather they selectively target axon-specific
390 mechanisms of growth. This observation extends previous reports demonstrating that the
391 organophosphorus pesticide chlorpyrifos (Howard *et al.*, 2005) and the NDL PCB 136 (Yang *et*
392 *al.*, 2014) differentially modulate axonal vs. dendritic growth.

393 In contrast to axon inhibition observed when primary hippocampal neurons were exposed to
394 BDE-47 or BDE-49 during the first 48 h in culture, exposure from DIV 7-9 did not inhibit axonal
395 growth, as quantified by western blot analyses of tau 1. This raises several considerations: (1)
396 western blotting does not have the sensitivity to detect subtle but significant differences in
397 axonal growth; (2) mature neurons are more resistant to the growth inhibitory effects of PBDEs;
398 or (3) PBDEs interfere with early stages of axonal morphogenesis. Our data provide direct
399 support for the third possibility: we observed that BDE 47 and BDE 49 delay the polarization of
400 hippocampal neurons. This was evident as a significant decrease at 48 h after plating in the
401 percentage of neurons exhibiting redistribution of GAP-43 into a single neurite that was
402 noticeably longer than the remaining “minor” neurites, marking its differentiation as the neuron’s
403 axon (Dotti *et al.*, 1988; Goslin *et al.*, 1990; Yamamoto *et al.*, 2012). This is in line with
404 previous studies demonstrating that MARCKS, an actin-binding protein enriched in axons that
405 co-distributes with GAP-43, is markedly decreased in rats exposed perinatally to BDE-71
406 (Kodavanti *et al.*, 2015; Ouimet *et al.*, 1990). Collectively, these observations support a model
407 in which PBDEs inhibit axonal growth, at least in part, by delaying neuronal polarization.

408 Neuronal polarization is controlled by $[Ca^{2+}]_i$, and Ca^{2+} ionophores completely suppress axon
409 formation in primary hippocampal neurons (Mattson *et al.*, 1990). Axonal growth requires an
410 optimal $[Ca^{2+}]_i$ in the axonal growth cone, and $[Ca^{2+}]_i$ levels on either side of this optimum inhibit
411 axonal growth (Kater and Mills, 1991). PBDEs have been shown to alter $[Ca^{2+}]_i$ in neurons via
412 mechanisms involving voltage-gated calcium channels, IP₃Rs and RyRs (Costa *et al.*, 2016;
413 Dingemans *et al.*, 2010a; Dingemans *et al.*, 2010b; Gassmann *et al.*, 2014; Kim *et al.*, 2011).
414 Pharmacological block of RyRs, but not L-type calcium channels or IP₃Rs, and siRNA

415 knockdown of RyR2 prevents BDE-47 and BDE-49 inhibition of axonal growth, suggesting that
416 these PBDEs inhibit axonal growth by sensitizing RyRs. Interestingly, RyR2 siRNA completely
417 blocks, while RyR1 siRNA only partially blocks, the axon inhibitory effects of BDE 47 and BDE
418 49. While immunohistochemical localization data indicate that both RyR isoforms are expressed
419 in axonal growth cones, the siRNA knockdown data suggest that RyR regulation of neuronal
420 polarity and/or axonal growth is isoform specific.

421 When considered in the context of previous reports that acute exposure to BDE-47 or BDE-
422 49 increases $[Ca^{2+}]_i$ in primary neurons (Dingemans et al., 2010a; Gassmann et al., 2014; Kim
423 et al., 2011), our data suggest a model in which RyR sensitization by BDE-47 or BDE-49 alters
424 local Ca^{2+} dynamics during early stages of axon development to move $[Ca^{2+}]_i$ away from the
425 optimal levels needed for axonal specification and/or growth. However, we were not able to
426 confirm this by documenting changes in $[Ca^{2+}]_i$ in either the soma or axonal growth cones of
427 primary hippocampal neurons exposed to BDE-47 or BDE-49 at concentrations that inhibit
428 axonal growth. We did observe significantly increased neuronal $[Ca^{2+}]_i$ in our model system
429 following acute exposure to PBDE concentrations comparable to those used in the studies cited
430 above, which were \geq 10-fold higher than those that inhibit axonal growth. It is possible that the
431 calcium fluorophore and/or imaging system we used are not sufficiently sensitive to detect
432 spatially or temporally restricted changes in $[Ca^{2+}]_i$ (Coburn *et al.*, 2008; Dingemans et al.,
433 2010a; Hong *et al.*, 2000; Mattson and Bruce-Keller, 1999). An alternative possibility is that
434 Ca^{2+} is not the primary mediator of the RyR-dependent effects of PBDEs on axonal growth.
435 Molecular effects of PBDEs other than Ca^{2+} dysregulation have been reported in experimental
436 models of developmental neurotoxicity, including thyroid hormone dysfunction, oxidative stress
437 and altered cholinergic, glutamatergic and GABAergic neurotransmission (Costa et al., 2014;
438 Hendriks and Westerink, 2015). Each of these molecular actions has been implicated in axonal
439 growth regulation (Goldberg, 2003), and RyR activity has been shown to either regulate or to be
440 regulated by each of these molecular actions (Pessah et al., 2010). Investigating potential roles

441 for these known molecular actions in RyR-dependent inhibition of axonal growth by PBDEs is
442 the focus of ongoing studies.

443 This study yielded several unexpected findings. First, the concentration-effect relationships of
444 BDE-47 and BDE-49 on axonal growth are comparable despite significant differences in their
445 potency at the RyR (Kim et al., 2011). One possibility is that astrocytes in the coculture
446 metabolize BDE-47 to hydroxylated forms previously shown to be potent RyR sensitizers (Kim
447 et al., 2011). Whether RyR-active BDE-47 metabolites are formed in these cocultures at levels
448 sufficient to influence axonal outgrowth has yet to be determined. An alternative possibility is
449 that the RyR is not the primary molecular target but rather a downstream effector. As discussed
450 above, Ca^{2+} -independent effects of PBDEs, including thyroid hormone dysfunction, oxidative
451 stress and altered neurotransmission (Costa et al., 2014; Hendriks and Westerink, 2015), have
452 been reported to modulate RyR activity (Pessah et al., 2010). This may also explain the second
453 surprising observation, which is that PBDEs and NDL-PCBs do not phenocopy each other's
454 effects on neuronal morphogenesis. As we previously demonstrated in primary hippocampal
455 neurons, NDL PCBs enhance dendritic growth via RyR-dependent mechanisms but have no
456 effect on axonal growth (Wayman et al., 2012b; Yang et al., 2014). In contrast, using the same
457 model system, we show here that BDE-47 and BDE-49 inhibit axonal growth via RyR-
458 dependent mechanisms but have no effect on dendritic arborization. If the RyR is an
459 intermediary signaling molecule rather than the primary molecular target for PBDEs, it would not
460 be surprising that they do not phenocopy NDL PCB effects on neuronal morphogenesis.
461 Alternatively, RyR activity is regulated by numerous accessory proteins (Pessah et al., 2010),
462 and NDL PCB interactions with the RyR require the presence of the FKBP12 accessory protein
463 (Samso et al., 2009; Wong et al., 1997b). While our earlier study suggests that PBDE
464 interactions with the RyR similarly require FKBP12 (Kim et al., 2011), possibly additional
465 accessory proteins are involved, and the profile of accessory proteins required for RyR
466 interactions differs between NDL PCBs and PBDEs. Since the complement of RyR accessory

467 proteins varies depending on the RyR isoform, and the subcellular compartment (Berridge,
468 2006; Pessah et al., 2010), this explanation would be consistent with our observation that both
469 RyR1 and RyR2 activity are required for the dendrite promoting activity of NDL PCBs (Wayman
470 et al., 2012b), while only RyR2 is required for the axon inhibiting effects of PBDEs. A related
471 possibility derives from observations that the kinetics of changes in $[Ca^{2+}]_i$ influence the profile
472 of activated downstream effectors (Berridge, 2006; Mattson, 1992). If the kinetics of PBDE
473 effects on RyR gating are different than those of NDL PCBs, they could activate unique
474 downstream effectors, resulting in differential effects on axons vs. dendrites. Future mechanistic
475 studies are warranted to distinguish the relative contributions of these possibilities to the distinct
476 toxicological profiles of PBDEs vs. NDL PCBs.

477 The human relevance of these *in vitro* mechanistic studies is suggested by the observation
478 that the effects BDE-47 and BDE-49 were observed at concentrations as low as 0.2 nM, which
479 are well within the range of PBDE plasma concentrations detected in highly exposed human
480 populations (Eskenazi et al., 2013; Eskenazi et al., 2011; Hertz-Picciotto et al., 2011). Whether
481 PBDE effects on axon growth contribute to neurobehavioral deficits associated with
482 developmental exposure remains to be determined. However, evidence that spatiotemporal
483 patterns in axonal growth can cause persistent changes in brain patterning and connectivity
484 (Berger-Sweeney and Hohmann, 1997; Cremer et al., 1997; Maier et al., 1999), and are linked
485 to neurodevelopmental disorders (Copf, 2016; Robichaux and Cowan, 2014), gives credence to
486 the possibility that inhibition of axonal growth is important in PBDE developmental neurotoxicity.

487

488 **Supplementary Data Description**

489 Supplemental files provide information regarding the synthesis and purity of FLA 365 (File S1),
490 representative phase contrast photomicrographs of cultures used for these studies (File S2),
491 and Ca^{2+} imaging data from cultures exposed acutely to BDE levels shown to inhibit axonal
492 growth (File S3).

493

494 **Funding Information**

495 This work was supported by the National Institute of Environmental Health Sciences [grant
496 numbers R01 ES014901, P01 ES011269, P42 ES04699, U54 HD079125, F32 ES024676 to
497 KMS, T32-MH073124 (postdoctoral fellowship) to KMS, and T32 ES007059 (predoctoral
498 fellowship) to HC], the United States Environmental Protection Agency [grant numbers
499 RD835550 and R83543201] and the J.B. Johnson Foundation [unrestricted gift to PJJ]. The
500 sponsors were not involved in the study design, the collection, analysis, and interpretation of
501 data, in the writing of the report or in the decision to submit the paper for publication.

502

503 **Acknowledgments**

504 The authors thank Dr. Kimberly P. Keil (UC Davis) and Dr. Keri A. Hayakawa (UC Davis) for
505 providing helpful feedback on early drafts of the manuscript.

506

507 **References**

508 Adasme T, Haeger P, Paula-Lima AC, Espinoza I, Casas-Alarcon MM, Carrasco MA, and Hidalgo C (2011).
509 Involvement of ryanodine receptors in neurotrophin-induced hippocampal synaptic plasticity and spatial
510 memory formation. *Proc Natl Acad Sci U S A* **108**(7), 3029-34.
511 Arie Y, Iketani M, Takamatsu K, Mikoshiba K, Goshima Y, and Takei K (2009). Developmental changes in
512 the regulation of calcium-dependent neurite outgrowth. *Biochem Biophys Res Commun* **379**(1), 11-5.
513 Behl M, Hsieh JH, Shafer TJ, Mundy WR, Rice JR, Boyd WA, Freedman JH, Hunter ES, 3rd, Jarema KA,
514 Padilla S, and Tice RR (2015). Use of alternative assays to identify and prioritize organophosphorus flame
515 retardants for potential developmental and neurotoxicity. *Neurotoxicol Teratol* **52**(Pt B), 181-93.
516 Berger-Sweeney J, and Hohmann CF (1997). Behavioral consequences of abnormal cortical
517 development: insights into developmental disabilities. *Behav Brain Res* **86**(2), 121-42.
518 Berridge MJ (2006). Calcium microdomains: organization and function. *Cell Calcium* **40**(5-6), 405-12.
519 Bradner JM, Suragh TA, and Caudle WM (2013). Alterations to the circuitry of the frontal cortex
520 following exposure to the polybrominated diphenyl ether mixture, DE-71. *Toxicology* **312**, 48-55.
521 Chandrasekaran V, Lea C, Sosa JC, Higgins D, and Lein PJ (2015). Reactive oxygen species are involved in
522 BMP-induced dendritic growth in cultured rat sympathetic neurons. *Mol Cell Neurosci* **67**, 116-25.
523 Chao HR, Tsou TC, Huang HL, and Chang-Chien GP (2011). Levels of breast milk PBDEs from southern
524 Taiwan and their potential impact on neurodevelopment. *Pediatr Res* **70**(6), 596-600.
525 Chen X, Huang C, Wang X, Chen J, Bai C, Chen Y, Chen X, Dong Q, and Yang D (2012). BDE-47 disrupts
526 axonal growth and motor behavior in developing zebrafish. *Aquat Toxicol* **120-121**, 35-44.

527 Chiesi M, Schwaller R, and Calviello G (1988). Inhibition of rapid Ca-release from isolated skeletal and
528 cardiac sarcoplasmic reticulum (SR) membranes. *Biochem Biophys Res Commun* **154**(1), 1-8.

529 Coburn CG, Curras-Collazo MC, and Kodavanti PR (2008). In vitro effects of environmentally relevant
530 polybrominated diphenyl ether (PBDE) congeners on calcium buffering mechanisms in rat brain.
531 *Neurochem Res* **33**(2), 355-64.

532 Copf T (2016). Impairments in dendrite morphogenesis as etiology for neurodevelopmental disorders
533 and implications for therapeutic treatments. *Neurosci Biobehav Rev* **68**, 946-978.

534 Costa LG, de Laat R, Tagliaferri S, and Pellacani C (2014). A mechanistic view of polybrominated diphenyl
535 ether (PBDE) developmental neurotoxicity. *Toxicol Lett* **230**(2), 282-94.

536 Costa LG, Tagliaferri S, Roque PJ, and Pellacani C (2016). Role of glutamate receptors in tetrabrominated
537 diphenyl ether (BDE-47) neurotoxicity in mouse cerebellar granule neurons. *Toxicol Lett* **241**, 159-66.

538 Cremer H, Chazal G, Goridis C, and Represa A (1997). NCAM is essential for axonal growth and
539 fasciculation in the hippocampus. *Mol Cell Neurosci* **8**(5), 323-35.

540 Dingemans MM, Heusinkveld HJ, Bergman A, van den Berg M, and Westerink RH (2010a). Bromination
541 pattern of hydroxylated metabolites of BDE-47 affects their potency to release calcium from intracellular
542 stores in PC12 cells. *Environ Health Perspect* **118**(4), 519-25.

543 Dingemans MM, van den Berg M, Bergman A, and Westerink RH (2010b). Calcium-related processes
544 involved in the inhibition of depolarization-evoked calcium increase by hydroxylated PBDEs in PC12 cells.
545 *Toxicol Sci* **114**(2), 302-9.

546 Dingemans MM, van den Berg M, and Westerink RH (2011). Neurotoxicity of brominated flame
547 retardants: (in)direct effects of parent and hydroxylated polybrominated diphenyl ethers on the
548 (developing) nervous system. *Environ Health Perspect* **119**(7), 900-7.

549 Dotti CG, Sullivan CA, and Banker GA (1988). The establishment of polarity by hippocampal neurons in
550 culture. *J Neurosci* **8**(4), 1454-68.

551 EFSA (2011). Scientific opinion on polybrominated diphenyl ethers (PBDEs) in food. *EFSA J.* **9**(2156), 274.

552 Eskenazi B, Chevrier J, Rauch SA, Kogut K, Harley KG, Johnson C, Trujillo C, Sjodin A, and Bradman A
553 (2013). In utero and childhood polybrominated diphenyl ether (PBDE) exposures and neurodevelopment
554 in the CHAMACOS study. *Environ Health Perspect* **121**(2), 257-62.

555 Eskenazi B, Fenster L, Castorina R, Marks AR, Sjodin A, Rosas LG, Holland N, Guerra AG, Lopez-Carillo L,
556 and Bradman A (2011). A comparison of PBDE serum concentrations in Mexican and Mexican-American
557 children living in California. *Environ Health Perspect* **119**(10), 1442-8.

558 Florvall L, Ask AL, Ogren SO, and Ross SB (1977). Selective monoamine oxidase inhibitors. *J Med Chem*
559 **21**, 56-63.

560 Gafni J, Munsch JA, Lam TH, Catlin MC, Costa LG, Molinski TF, and Pessah IN (1997). Xestospongins:
561 potent membrane permeable blockers of the inositol 1,4,5-trisphosphate receptor. *Neuron* **19**(3), 723-
562 33.

563 Gascon M, Fort M, Martinez D, Carsin AE, Fornis J, Grimalt JO, Santa Marina L, Lertxundi N, Sunyer J, and
564 Vrijheid M (2012). Polybrominated diphenyl ethers (PBDEs) in breast milk and neuropsychological
565 development in infants. *Environ Health Perspect* **120**(12), 1760-5.

566 Gassmann K, Schreiber T, Dingemans MM, Krause G, Roderigo C, Giersiefer S, Schuwald J, Moors M,
567 Unfried K, Bergman A, Westerink RH, Rose CR, and Fritsche E (2014). BDE-47 and 6-OH-BDE-47 modulate
568 calcium homeostasis in primary fetal human neural progenitor cells via ryanodine receptor-independent
569 mechanisms. *Arch Toxicol* **88**(8), 1537-48.

570 Goldberg JL (2003). How does an axon grow? *Genes Dev* **17**(8), 941-58.

571 Gomez TM, Snow DM, and Letourneau PC (1995). Characterization of spontaneous calcium transients in
572 nerve growth cones and their effect on growth cone migration. *Neuron* **14**(6), 1233-46.

573 Goslin K, and Banker G (1990). Rapid changes in the distribution of GAP-43 correlate with the expression
574 of neuronal polarity during normal development and under experimental conditions. *J Cell Biol* **110**(4),
575 1319-31.

576 Goslin K, Schreyer DJ, Skene JH, and Banker G (1990). Changes in the distribution of GAP-43 during the
577 development of neuronal polarity. *J Neurosci* **10**(2), 588-602.

578 Harrill JA, Freudenrich TM, Robinette BL, and Mundy WR (2011). Comparative sensitivity of human and
579 rat neural cultures to chemical-induced inhibition of neurite outgrowth. *Toxicol Appl Pharmacol* **256**(3),
580 268-80.

581 Harrill JA, Robinette BL, Freudenrich T, and Mundy WR (2013). Use of high content image analyses to
582 detect chemical-mediated effects on neurite sub-populations in primary rat cortical neurons.
583 *Neurotoxicology* **34**, 61-73.

584 Hayashi K, Kawai-Hirai R, Ishikawa K, and Takata K (2002). Reversal of neuronal polarity characterized by
585 conversion of dendrites into axons in neonatal rat cortical neurons in vitro. *Neuroscience* **110**(1), 7-17.

586 Hendriks HS, and Westerink RH (2015). Neurotoxicity and risk assessment of brominated and alternative
587 flame retardants. *Neurotoxicol Teratol* **52**(Pt B), 248-69.

588 Herbstman JB, Sjodin A, Kurzon M, Lederman SA, Jones RS, Rauh V, Needham LL, Tang D, Niedzwiecki M,
589 Wang RY, and Perera F (2010). Prenatal exposure to PBDEs and neurodevelopment. *Environ Health*
590 *Perspect* **118**(5), 712-9.

591 Hertle DN, and Yeckel MF (2007). Distribution of inositol-1,4,5-trisphosphate receptor isoforms and
592 ryanodine receptor isoforms during maturation of the rat hippocampus. *Neuroscience* **150**(3), 625-38.

593 Hertz-Picciotto I, Bergman A, Fangstrom B, Rose M, Krakowiak P, Pessah I, Hansen R, and Bennett DH
594 (2011). Polybrominated diphenyl ethers in relation to autism and developmental delay: a case-control
595 study. *Environ Health* **10**(1), 1.

596 Hoffman K, Adgent M, Goldman BD, Sjodin A, and Daniels JL (2012). Lactational exposure to
597 polybrominated diphenyl ethers and its relation to social and emotional development among toddlers.
598 *Environ Health Perspect* **120**(10), 1438-42.

599 Hong K, Nishiyama M, Henley J, Tessier-Lavigne M, and Poo M (2000). Calcium signalling in the guidance
600 of nerve growth by netrin-1. *Nature* **403**(6765), 93-8.

601 Howard AS, Bucelli R, Jett DA, Bruun D, Yang D, and Lein PJ (2005). Chlorpyrifos exerts opposing effects
602 on axonal and dendritic growth in primary neuronal cultures. *Toxicol Appl Pharmacol* **207**(2), 112-24.

603 Inglefield JR, Mundy WR, and Shafer TJ (2001). Inositol 1,4,5-triphosphate receptor-sensitive Ca(2+)
604 release, store-operated Ca(2+) entry, and cAMP responsive element binding protein phosphorylation in
605 developing cortical cells following exposure to polychlorinated biphenyls. *J Pharmacol Exp Ther* **297**(2),
606 762-73.

607 Jacques-Fricke BT, Seow Y, Gottlieb PA, Sachs F, and Gomez TM (2006). Ca²⁺ influx through
608 mechanosensitive channels inhibits neurite outgrowth in opposition to other influx pathways and
609 release from intracellular stores. *J Neurosci* **26**(21), 5656-64.

610 Kapfhammer JP (2004). Cellular and molecular control of dendritic growth and development of
611 cerebellar Purkinje cells. *Prog Histochem Cytochem* **39**(3), 131-82.

612 Kater SB, and Mills LR (1991). Regulation of growth cone behavior by calcium. *J Neurosci* **11**(4), 891-9.

613 Keith RA, Mangano TJ, DeFeo PA, Ernst GE, and Warawa EJ (1994). Differential inhibition of neuronal
614 calcium entry and [3H]-D-aspartate release by the quaternary derivatives of verapamil and emopamil. *Br*
615 *J Pharmacol* **113**(2), 379-84.

616 Kim KH, Bose DD, Ghogha A, Riehl J, Zhang R, Barnhart CD, Lein PJ, and Pessah IN (2011). Para- and
617 ortho-substitutions are key determinants of polybrominated diphenyl ether activity toward ryanodine
618 receptors and neurotoxicity. *Environ Health Perspect* **119**(4), 519-26.

619 Kodavanti PR, and Curras-Collazo MC (2010). Neuroendocrine actions of organohalogen: thyroid
620 hormones, arginine vasopressin, and neuroplasticity. *Front Neuroendocrinol* **31**(4), 479-96.

621 Kodavanti PR, Royland JE, Osorio C, Winnik WM, Ortiz P, Lei L, Ramabhadran R, and Alzate O (2015).
622 Developmental exposure to a commercial PBDE mixture: effects on protein networks in the cerebellum
623 and hippocampus of rats. *Environ Health Perspect* **123**(5), 428-36.

624 Kodavanti PR, Shafer TJ, Ward TR, Mundy WR, Freudenrich T, Harry GJ, and Tilson HA (1994). Differential
625 effects of polychlorinated biphenyl congeners on phosphoinositide hydrolysis and protein kinase C
626 translocation in rat cerebellar granule cells. *Brain Res* **662**(1-2), 75-82.

627 Lein PJ, Banker GA, and Higgins D (1992). Laminin selectively enhances axonal growth and accelerates
628 the development of polarity by hippocampal neurons in culture. *Brain Res Dev Brain Res* **69**(2), 191-7.

629 Lobner D (2000). Comparison of the LDH and MTT assays for quantifying cell death: validity for neuronal
630 apoptosis? *J Neurosci Methods* **96**(2), 147-52.

631 Lohmann C, and Wong RO (2005). Regulation of dendritic growth and plasticity by local and global
632 calcium dynamics. *Cell Calcium* **37**(5), 403-9.

633 Lunder S, Hovander L, Athanassiadis I, and Bergman A (2010). Significantly higher polybrominated
634 diphenyl ether levels in young U.S. children than in their mothers. *Environ Sci Technol* **44**(13), 5256-62.

635 Mack WM, Zimanyi I, and Pessah IN (1992). Discrimination of multiple binding sites for antagonists of
636 the calcium release channel complex of skeletal and cardiac sarcoplasmic reticulum. *J Pharmacol Exp
637 Ther* **262**(3), 1028-37.

638 Maier DL, Mani S, Donovan SL, Soppet D, Tessarollo L, McCasland JS, and Meiri KF (1999). Disrupted
639 cortical map and absence of cortical barrels in growth-associated protein (GAP)-43 knockout mice. *Proc
640 Natl Acad Sci U S A* **96**(16), 9397-402.

641 Mattson MP (1992). Calcium as sculptor and destroyer of neural circuitry. *Exp Gerontol* **27**(1), 29-49.

642 Mattson MP, and Bruce-Keller AJ (1999). Compartmentalization of signaling in neurons: evolution and
643 deployment. *J Neurosci Res* **58**(1), 2-9.

644 Mattson MP, Murain M, and Guthrie PB (1990). Localized calcium influx orients axon formation in
645 embryonic hippocampal pyramidal neurons. *Brain Res Dev Brain Res* **52**(1-2), 201-9.

646 Meijering E, Jacob M, Sarria JC, Steiner P, Hirling H, and Unser M (2004). Design and validation of a tool
647 for neurite tracing and analysis in fluorescence microscopy images. *Cytometry A* **58**(2), 167-76.

648 Miller MF, Chernyak SM, Batterman S, and Loch-Carusio R (2009). Polybrominated diphenyl ethers in
649 human gestational membranes from women in southeast Michigan. *Environ Sci Technol* **43**(9), 3042-6.

650 Mosmann T (1983). Rapid colorimetric assay for cellular growth and survival: application to proliferation
651 and cytotoxicity assays. *J Immunol Methods* **65**(1-2), 55-63.

652 Ohashi R, Sakata S, Naito A, Hirashima N, and Tanaka M (2014). Dendritic differentiation of cerebellar
653 Purkinje cells is promoted by ryanodine receptors expressed by Purkinje and granule cells. *Dev Neurobiol*
654 **74**(4), 467-80.

655 Ooashi N, Futatsugi A, Yoshihara F, Mikoshiba K, and Kamiguchi H (2005). Cell adhesion molecules
656 regulate Ca²⁺-mediated steering of growth cones via cyclic AMP and ryanodine receptor type 3. *J Cell
657 Biol* **170**(7), 1159-67.

658 Ostrovskaya O, Goyal R, Osman N, McAllister CE, Pessah IN, Hume JR, and Wilson SM (2007). Inhibition
659 of ryanodine receptors by 4-(2-aminopropyl)-3,5-dichloro-N,N-dimethylaniline (FLA 365) in canine
660 pulmonary arterial smooth muscle cells. *J Pharmacol Exp Ther* **323**(1), 381-90.

661 Ouimet CC, Wang JK, Walaas SI, Albert KA, and Greengard P (1990). Localization of the MARCKS (87 kDa)
662 protein, a major specific substrate for protein kinase C, in rat brain. *J Neurosci* **10**(5), 1683-98.

663 Pessah IN, Cherednichenko G, and Lein PJ (2010). Minding the calcium store: Ryanodine receptor
664 activation as a convergent mechanism of PCB toxicity. *Pharmacol Ther* **125**(2), 260-85.

665 Robichaux MA, and Cowan CW (2014). Signaling mechanisms of axon guidance and early
666 synaptogenesis. *Curr Top Behav Neurosci* **16**, 19-48.

667 Roze E, Meijer L, Bakker A, Van Braeckel KN, Sauer PJ, and Bos AF (2009). Prenatal exposure to
668 organohalogens, including brominated flame retardants, influences motor, cognitive, and behavioral
669 performance at school age. *Environ Health Perspect* **117**(12), 1953-8.

670 Samso M, Feng W, Pessah IN, and Allen PD (2009). Coordinated movement of cytoplasmic and
671 transmembrane domains of RyR1 upon gating. *PLoS Biol* **7**(4), e85.

672 Seymour-Laurent KJ, and Barish ME (1995). Inositol 1,4,5-trisphosphate and ryanodine receptor
673 distributions and patterns of acetylcholine- and caffeine-induced calcium release in cultured mouse
674 hippocampal neurons. *J Neurosci* **15**(4), 2592-608.

675 She J, Holden A, Sharp M, Tanner M, Williams-Derry C, and Hooper K (2007). Polybrominated diphenyl
676 ethers (PBDEs) and polychlorinated biphenyls (PCBs) in breast milk from the Pacific Northwest.
677 *Chemosphere* **67**(9), S307-17.

678 Shy CG, Huang HL, Chang-Chien GP, Chao HR, and Tsou TC (2011). Neurodevelopment of infants with
679 prenatal exposure to polybrominated diphenyl ethers. *Bull Environ Contam Toxicol* **87**(6), 643-8.

680 Stamou M, Streifel KM, Goines PE, and Lein PJ (2013). Neuronal connectivity as a convergent target of
681 gene x environment interactions that confer risk for Autism Spectrum Disorders. *Neurotoxicol Teratol*
682 **36**, 3-16.

683 Toms LM, Sjodin A, Harden F, Hobson P, Jones R, Edenfield E, and Mueller JF (2009). Serum
684 polybrominated diphenyl ether (PBDE) levels are higher in children (2-5 years of age) than in infants and
685 adults. *Environ Health Perspect* **117**(9), 1461-5.

686 USEPA (2010). An Exposure Assessment of Polybrominated Diphenyl Ethers. 378.

687 Valnegri P, Puram SV, and Bonni A (2015). Regulation of dendrite morphogenesis by extrinsic cues.
688 *Trends Neurosci* **38**(7), 439-47.

689 Vaughan PJ, Pike CJ, Cotman CW, and Cunningham DD (1995). Thrombin receptor activation protects
690 neurons and astrocytes from cell death produced by environmental insults. *J Neurosci* **15**(7 Pt 2), 5389-
691 401.

692 Wayman GA, Bose DD, Yang D, Lesiak A, Bruun D, Impey S, Ledoux V, Pessah IN, and Lein PJ (2012a).
693 PCB-95 modulates the calcium-dependent signaling pathway responsible for activity-dependent
694 dendritic growth. *Environ Health Perspect* **120**(7), 1003-9.

695 Wayman GA, Impey S, Marks D, Saneyoshi T, Grant WF, Derkach V, and Soderling TR (2006). Activity-
696 dependent dendritic arborization mediated by CaM-kinase I activation and enhanced CREB-dependent
697 transcription of Wnt-2. *Neuron* **50**(6), 897-909.

698 Wayman GA, Yang D, Bose DD, Lesiak A, Ledoux V, Bruun D, Pessah IN, and Lein PJ (2012b). PCB-95
699 promotes dendritic growth via ryanodine receptor-dependent mechanisms. *Environ Health Perspect*
700 **120**(7), 997-1002.

701 Welshhans K, and Rehder V (2007). Nitric oxide regulates growth cone filopodial dynamics via ryanodine
702 receptor-mediated calcium release. *Eur J Neurosci* **26**(6), 1537-47.

703 Wiggin GR, Fawcett JP, and Pawson T (2005). Polarity proteins in axon specification and synaptogenesis.
704 *Dev Cell* **8**(6), 803-16.

705 Wong PW, Brackney WR, and Pessah IN (1997a). Ortho-substituted polychlorinated biphenyls alter
706 microsomal calcium transport by direct interaction with ryanodine receptors of mammalian brain. *J Biol*
707 *Chem* **272**(24), 15145-53.

708 Wong PW, Joy RM, Albertson TE, Schantz SL, and Pessah IN (1997b). Ortho-substituted 2,2',3,5',6-
709 pentachlorobiphenyl (PCB 95) alters rat hippocampal ryanodine receptors and neuroplasticity in vitro:
710 evidence for altered hippocampal function. *Neurotoxicology* **18**(2), 443-56.

711 Wong PW, and Pessah IN (1996). Ortho-substituted polychlorinated biphenyls alter calcium regulation
712 by a ryanodine receptor-mediated mechanism: structural specificity toward skeletal- and cardiac-type
713 microsomal calcium release channels. *Mol Pharmacol* **49**(4), 740-51.

714 Yamamoto H, Demura T, Morita M, Banker GA, Tanii T, and Nakamura S (2012). Differential neurite
715 outgrowth is required for axon specification by cultured hippocampal neurons. *J Neurochem* **123**(6),
716 904-10.
717 Yang D, Kania-Korwel I, Ghogha A, Chen H, Stamou M, Bose DD, Pessah IN, Lehmler HJ, and Lein PJ
718 (2014). PCB 136 atropselectively alters morphometric and functional parameters of neuronal
719 connectivity in cultured rat hippocampal neurons via ryanodine receptor-dependent mechanisms.
720 *Toxicol Sci* **138**(2), 379-92.
721 Yang D, Kim KH, Phimister A, Bachstetter AD, Ward TR, Stackman RW, Mervis RF, Wisniewski AB, Klein
722 SL, Kodavanti PR, Anderson KA, Wayman G, Pessah IN, and Lein PJ (2009). Developmental exposure to
723 polychlorinated biphenyls interferes with experience-dependent dendritic plasticity and ryanodine
724 receptor expression in weanling rats. *Environ Health Perspect* **117**(3), 426-35.
725 Zheng JQ, and Poo MM (2007). Calcium signaling in neuronal motility. *Annu Rev Cell Dev Biol* **23**, 375-
726 404.

727

728 **Figure Legends**

729

730 **Figure 1.** BDE-47 and BDE-49 do not alter dendritic growth in cultured hippocampal neurons.
731 Cells dissociated from postnatal day 1 (P1) rat hippocampi were transfected with MAP2B-eGFP
732 at day *in vitro* (DIV) 6. On DIV 7, cultures were exposed to vehicle (DMSO diluted 1:1000) or
733 varying concentrations of BDE-47 or BDE-49 for 48 h. (A) Representative photomicrographs of
734 DIV 9 neurons expressing MAP2B-eGFP following exposure to vehicle, BDE-47 (200 nM) or
735 BDE-49 (200 nM). PCB 95 (200 nM) was added to a subset of cultures as a positive control. (B)
736 Quantification of dendritic length in GFP+ neurons. Data from one experiment presented as the
737 mean \pm SE (n=30-40 neurons per condition from 3 cultures in one independent dissection).
738 Experiments were repeated in 3 independent dissections with comparable results from each
739 experiment. *p<0.05 relative to vehicle control. Scale bar = 25 μ m.

740

741 **Figure 2.** BDE-47 and BDE-49 reduce axon length in cultured hippocampal neurons. Cells
742 dissociated from P1 rat hippocampi were exposed to vehicle or varying concentrations of BDE-
743 47 or BDE-49 beginning 3 h after plating. After a 48 h exposure, neurons (DIV 2) were fixed and
744 immunostained for Tau-1. (A) Representative photomicrographs of DIV 2 hippocampal neurons

745 exposed to vehicle, BDE-47 (200 nM) or BDE-49 (200 nM). (B) Quantification of axon length in
746 Tau-1 immunopositive cells. Data presented as the mean \pm SE (n=70-90 neurons from 3
747 independent dissections in all groups except for the 20 pM group in which n=40 neurons from 3
748 independent dissections). **p<0.01, ***p<0.001 relative to vehicle control. Scale bar = 10 μ m.

749

750 **Figure 3.** BDE-47 and BDE-49 are not cytotoxic at concentrations that decrease axon length.
751 LDH release into the media (A) and live-dead staining using calcein AM and propidium iodide
752 (B) were used to assess cell viability in dissociated hippocampal cultures on DIV 2 following a
753 48 h exposure to vehicle or varying concentrations of BDE 47 or BDE 49. 0.1% Triton X-100
754 was used as a positive control. Data presented as mean \pm SE (n=3 independent dissections).
755 *p<0.05, ***p<0.0001 relative to vehicle control.

756

757 **Figure 4.** BDE-47 and BDE-49 do not decrease tau-1 expression in mature cultures. At DIV 5,
758 hippocampal neurons were treated with BDE-47 (A) or BDE-49 (B) for 48 h. Sodium
759 orthovanadate (30 μ M) was used as a positive control (Harrill *et al.*, 2011). At the end of the
760 exposure, cells were lysed for western blotting and probed with antibodies specific for tau-1
761 (axonal cytoskeletal protein) and GAPDH (loading control) as shown in representative western
762 blots (top panels). Bar graphs (bottom panel) represent densitometric data. Densitometric
763 values of tau-1 immunopositive bands were normalized to densitometric values for GAPDH
764 immunopositive bands within the same sample. Data presented as mean \pm SE (n=4
765 independent dissections). ***p<0.001 relative to vehicle control.

766

767 **Figure 5.** BDE-47 and BDE-49 delay the development of polarity in hippocampal neurons.
768 Polarity was quantified in dissociated hippocampal cell cultures based on the subcellular
769 distribution of GAP-43 immunoreactivity and morphometric criteria. (A) Representative
770 photomicrographs of hippocampal neurons at different stages of polarization. (B) Ontogeny of

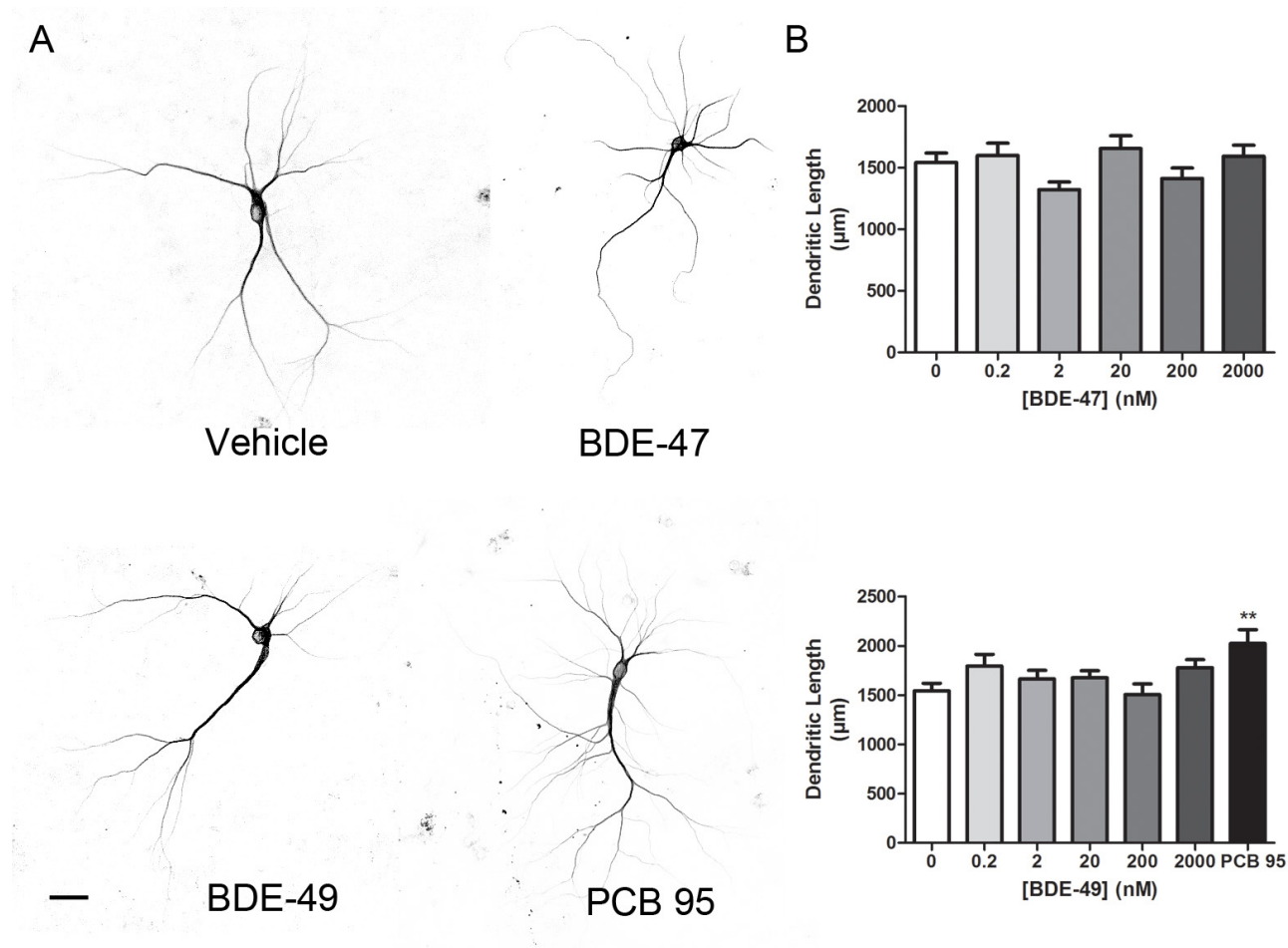
771 polarity in hippocampal cultures grown under the culture conditions used in this study. (C)
772 Percent of polarized (Stage 3) neurons at DIV 2 following a 48 h exposure to vehicle, BDE-47
773 (200 nM) or BDE-49 (200 nM). Data presented as mean \pm SE (n=9 coverslips collected from 3
774 independent dissections, 70-150 neurons each coverslip). *p<0.05 relative to vehicle control.
775 Scale bar = 10 μ m.

776
777 **Figure 6.** Acute exposure to BDE-47 and BDE-49 increases $[Ca^{2+}]_i$ in cultured hippocampal
778 neurons. DIV 2 hippocampal cultures were loaded with Fluo-4AM (4 μ M) and imaged for 26 min
779 to quantify spontaneous calcium transients. (A) Combined traces of neuronal responses to
780 vehicle (n=69), 20 μ M BDE-47 (n=57) or 20 μ M BDE-49 (n=49). Arrow indicates when PBDE or
781 vehicle were added to the culture, typically after 5 min of baseline recording. Bar graphs at the
782 right summarize the maximal amplitude of the Ca^{2+} signal normalized to baseline (F/F₀) and the
783 area under the curve (AUC) of signal above the baseline amplitude in the neuronal cell soma
784 (B) and growth cones (C). Data presented as mean \pm SE (n=4 independent dissections).
785 *p<0.05, ***p<0.0001 relative to vehicle control.

786
787 **Figure 7.** Pharmacological block of RyR Ca^{2+} channels prevents the inhibitory effects of BDE-47
788 or BDE-49 on axon length. Dissociated hippocampal cell cultures were pre-treated with the L-
789 type Ca^{2+} channel blocker verapamil (30 μ M), the IP₃ receptor blocker xestospongine C (1 μ M) or
790 the RyR blocker FLA365 (10 μ M) 30 min prior to addition of vehicle, BDE-47 (200 nM) or BDE-
791 49 (200 nM). After 48 h, cultures were fixed and immunostained for Tau-1. Axon length was
792 quantified in cultures treated with pharmacological inhibitors in the absence (A) or presence (B)
793 of BDEs. Data presented as the mean \pm SE (n=30-60 neurons each condition from 3 cultures
794 derived from a single dissection). This experiment was repeated in culture derived from 3
795 independent dissections with comparable results. *p<0.05 relative to vehicle control, #p<0.05
796 relative to BDE-matched cultures not treated with a pharmacological inhibitor.

797

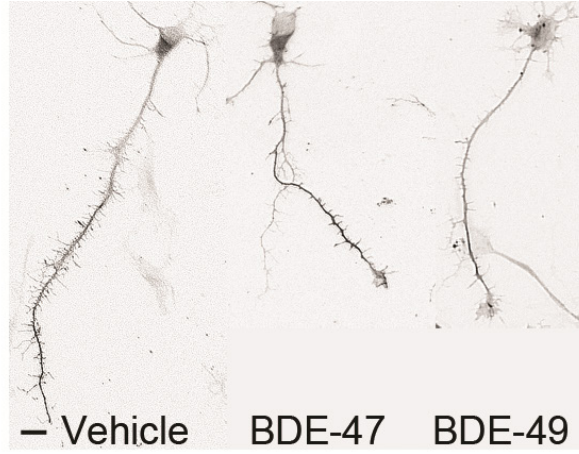
798 **Figure 8.** BDE-47 and BDE-49 reduce axon length via RyR2-dependent mechanism(s). (A)
799 Representative photomicrographs of axonal growth cones in DIV 2 hippocampal cultures co-
800 labeled with fluorescently tagged phalloidin (green) and antibody selective for RyR1 (red, left) or
801 RyR2 (red, right). (B) Quantitative analyses of axonal length in Cy5 positive neurons.
802 Dissociated hippocampal cells were electroporated with Cy5-labeled scrambled (control), RYR1
803 or RYR2 siRNA prior to plating. Data presented as the mean \pm SE (n=90 neurons collected from
804 3 independent dissections). *p<0.05 relative to vehicle control, #p<0.05 relative to cultures
805 transfected with control siRNA and exposed to the same BDE. Scale bar = 5 μ m.



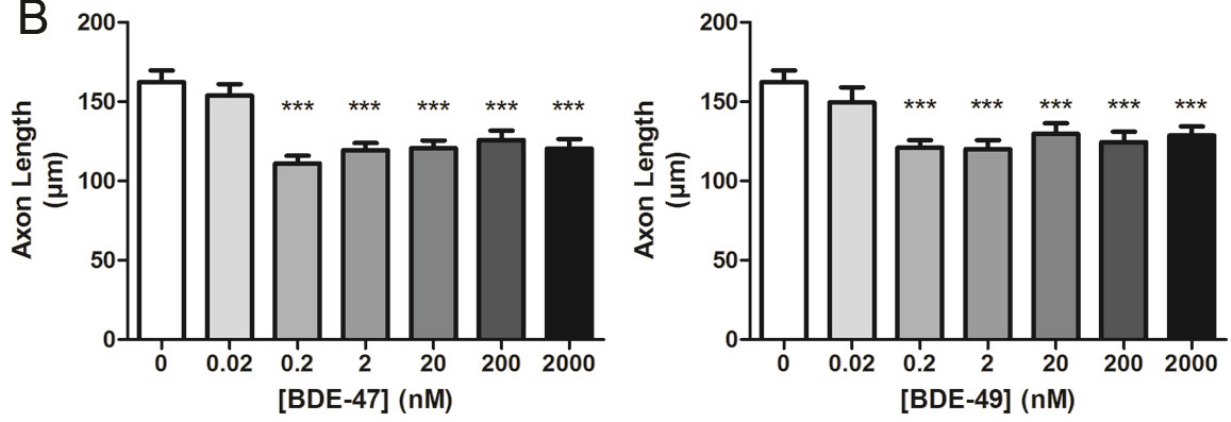
806

807 **Figure 1.**

A

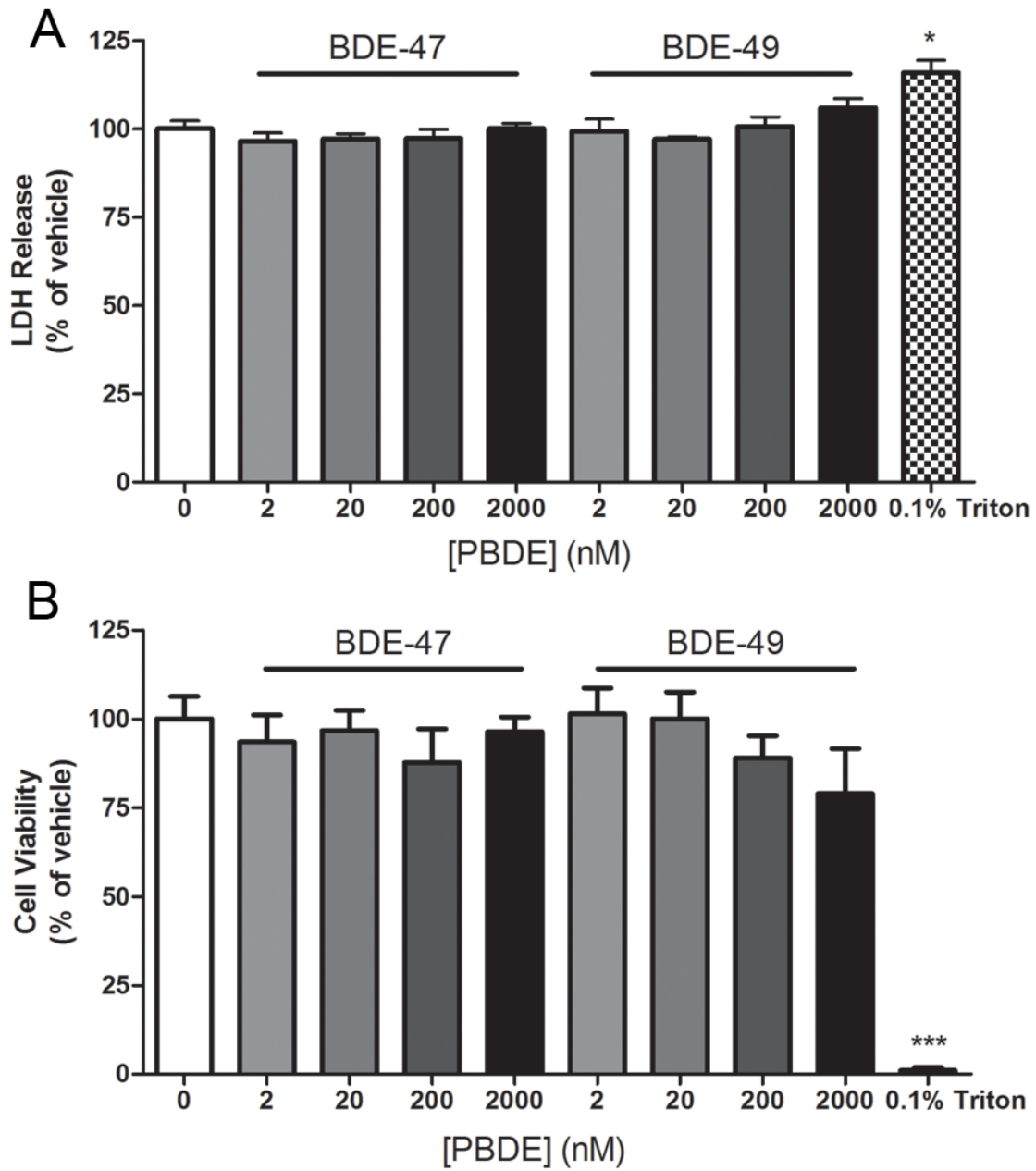


B



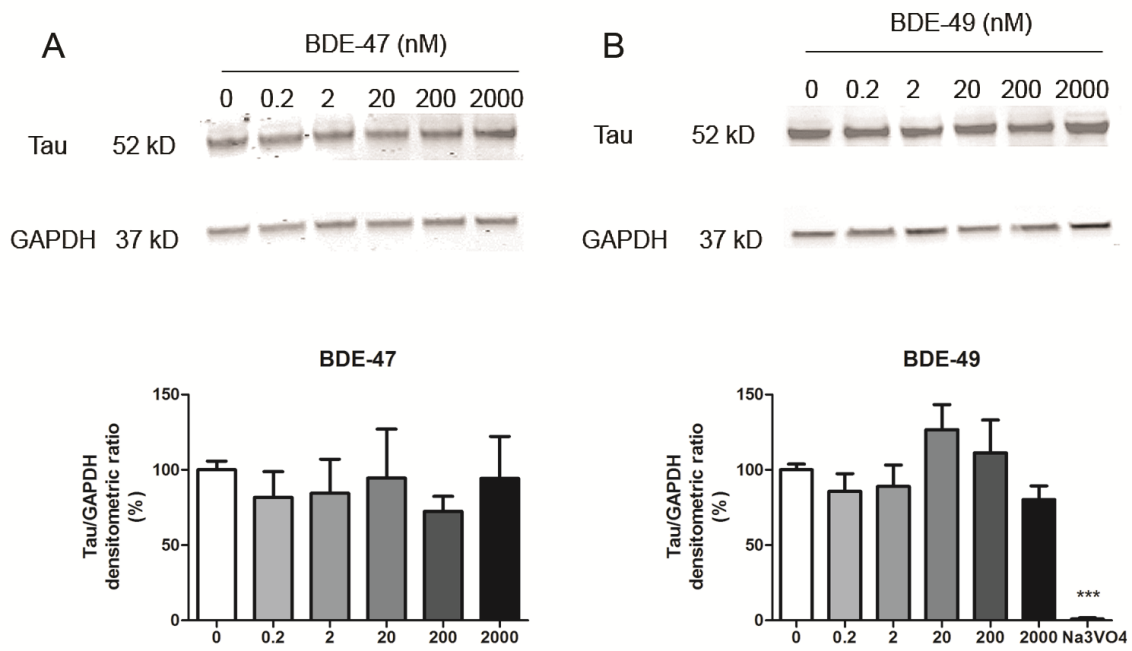
808

809 **Figure 2.**



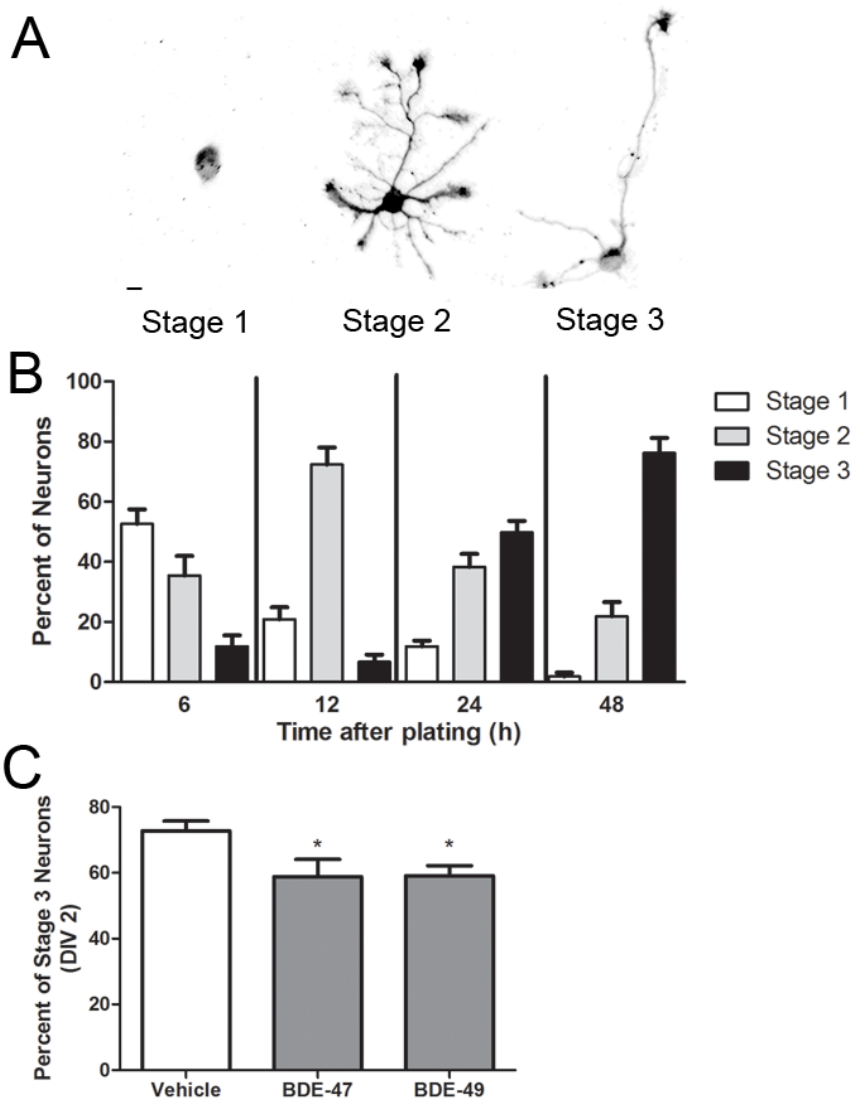
810

811 **Figure 3.**



812

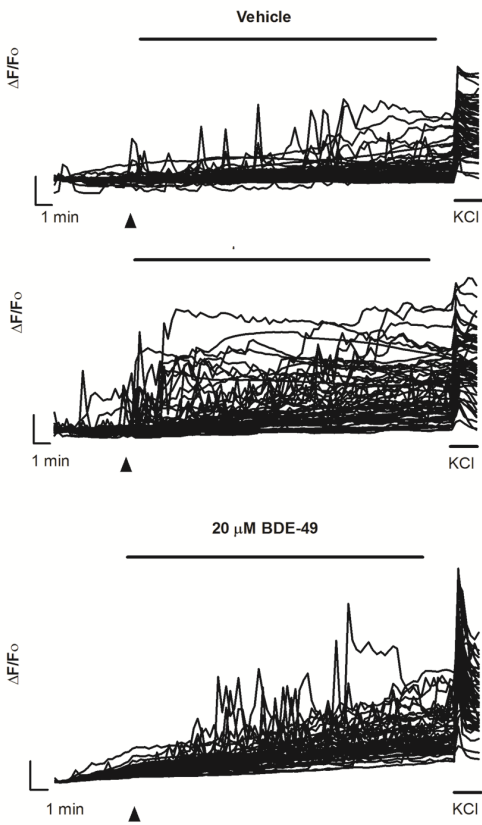
813 **Figure 4.**



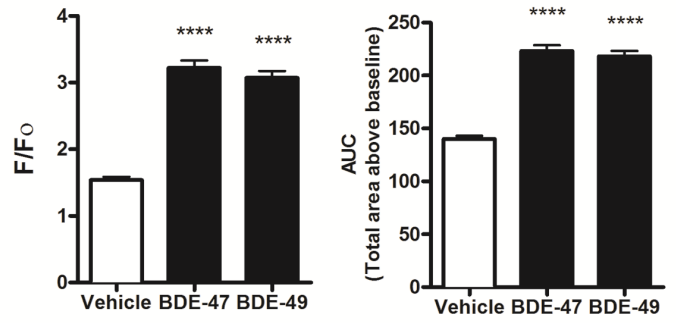
814

815 **Figure 5.**

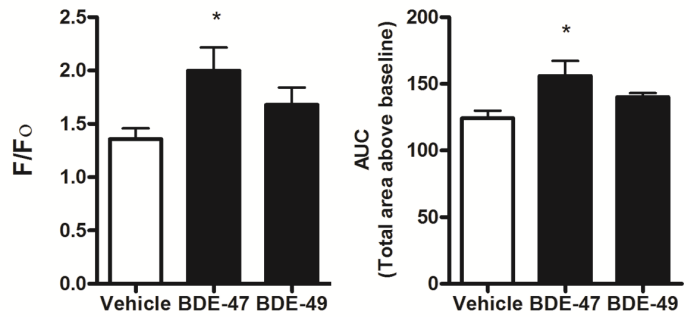
A Cell Soma



B Cell Soma



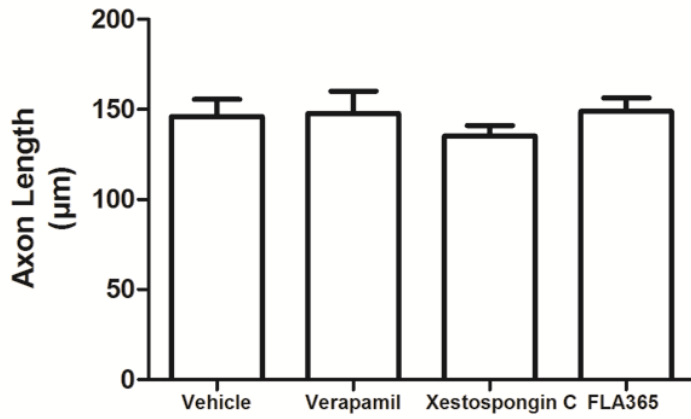
C Growth Cone



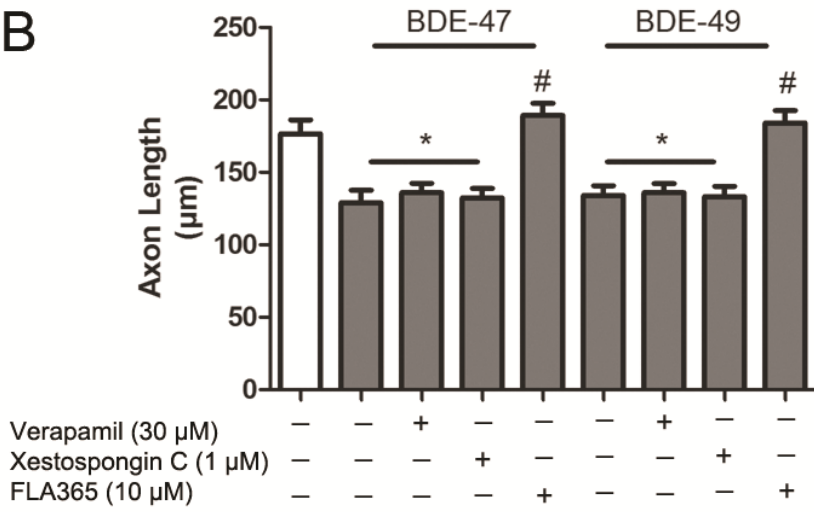
816

817 **Figure 6.**

A

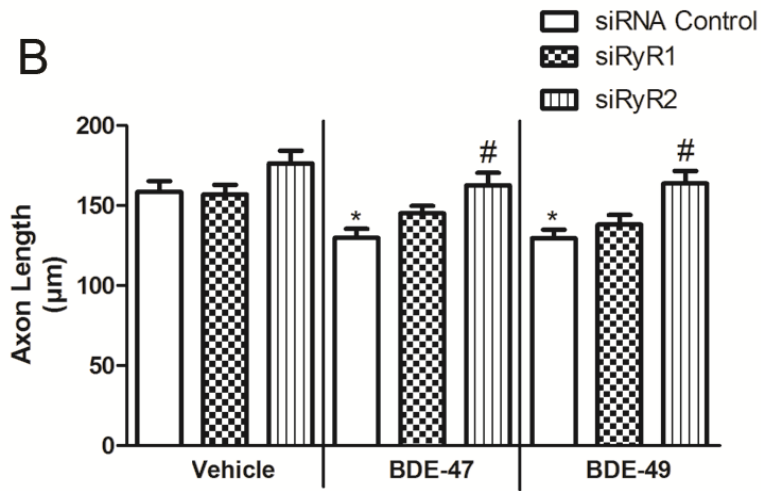
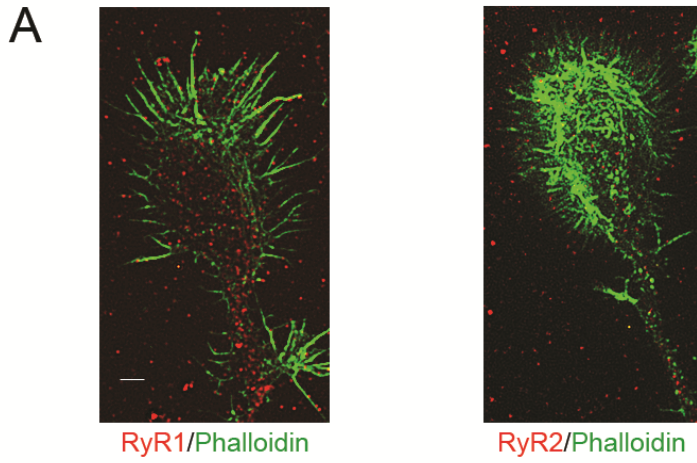


B



818

819 **Figure 7.**



820

821 **Figure 8.**